

Article

# A Unified Approach for Analysis of Faults in Different Configurations of PV Arrays and Its Impact on Power Grid

Saba Gul <sup>1</sup>, Azhar Ul Haq <sup>1,\*</sup>, Marium Jalal <sup>2,3</sup>, Almas Anjum <sup>1</sup> and Ihsan Ullah Khalil <sup>1</sup> 

<sup>1</sup> Department of Electrical Engineering, NUST College of E&ME, National University of Sciences and Technology (NUST), Rawalpindi 46000, Pakistan; sb101tahirgul@gmail.com (S.G.); almas.anjum@yahoo.com (A.A.); iukhalil211@gmail.com (I.U.K.)

<sup>2</sup> Department of Electronic Engineering, Fatima Jinnah Women University, Rawalpindi 46000, Pakistan; mariumjalal@fjwu.edu.pk

<sup>3</sup> Department of Electrical Engineering, Lahore College for Women University(LCWU), Lahore 54000, Pakistan

\* Correspondence: azhar.ulhaq@ceme.nust.edu.pk

Received: 17 September 2019; Accepted: 11 October 2019; Published: 28 December 2019



**Abstract:** Fault analysis in photovoltaic (PV) arrays is considered important for improving the safety and efficiency of a PV system. Faults do not only reduce efficiency but are also detrimental to the life span of a system. Output can be greatly affected by PV technology, configuration, and other operating conditions. Thus, it is important to consider the impact of different PV configurations and materials for thorough analysis of faults. This paper presents a detailed investigation of faults including non-uniform shading, open circuit and short circuit in different PV interconnections including Series-Parallel (SP), Honey-Comb (HC) and Total-cross-Tied (TCT). A special case of multiple faults in PV array under non-uniform irradiance is also investigated to analyze their combined impact on considered different PV interconnections. In order to be more comprehensive, we have considered monocrystalline and thin-film PV to analyze faults and their impact on power grids. Simulations are conducted in MATLAB/Simulink, and the obtained results in terms of power(P)–voltage(V) curve are compared and discussed. It is found that utilization of thin-film PV technology with appropriated PV interconnections can minimize the impact of faults on a power grid with improved performance of the system.

**Keywords:** photovoltaic; PV arrays; PV faults; PV interconnections; Total Cross Tied; PV configurations; power grid; P-V curve

## 1. Introduction

Rapid growth in the deployment of renewable energy has been witnessed over the past few years despite it being less efficient and more susceptible to unexpected faults [1]. Advancement in PV technology is still restricted due to high cost arising from its low efficiency and high probability of fault occurrence during photovoltaic system operation. The most commonly used crystalline silicon PV material has up to ~27% efficiency under normal operating conditions [2]. The efficiency of a PV system can be greatly reduced due to various factors such as degradation of the PV module and wiring losses including open circuit; short circuit faults; and severe shading through obstruction of trees, buildings, bird dropping, and heavy dust layer accumulation on PV panel [3].

A study on monitoring of PV arrays in 2010 showed that faults can reduce the generated power of solar systems annually by about 18.9% [4]. The faults in large PV systems are difficult to spot and can remain undetected, leading to higher risks of arc faults. Many fire accidents have been reported in the past [5]. One such event happened in Bakersfield, California in 2009 due to undetected

ground faults which led towards a large fire accident [6]. Another similar accident happened due to undetected faults in a 1 MW PV system of Mount Halley, North Carolina in 2011 [7]. Thus, timely diagnosis of faults in PV systems is very important for the prevention of such large fire accidents [8]. The modeling of a PV system under electrical faults [9] has been studied in the literature [10]. A review of faults in PV systems is presented in [11]. Power generation is also dependent upon the type of PV material [12]. The impact of shading on different PV technologies [13] has been largely investigated in the past [14–18]. The performance of crystalline PV material can be affected greatly by environmental conditions [14]. P-V curve analysis for studying the impact of shading on polycrystalline and thin-film PV modules was performed in [15]. Thin-film PV performed better as compared to polycrystalline PV under severe shading in terms of power output. The experimental analysis of PV material in Anatolia also proved that thin-film technology has less impact on shading and high temperature as compared to crystalline PV material [16]. Only shading and temperature conditions are analyzed for thin-film PV technology [17]. Further research is needed to investigate the impact of short circuit and open circuit faults on thin-film PV technology.

Different methods of maximum power point tracking (MPPT) [18] have been investigated but improvements in the algorithm cannot compensate for significant power losses that occur through fault occurrence in PV arrays. A reconfiguration technique was adopted in [19] to increase power generation but this technique requires a complex switching matrix with many sensors and proper control algorithms for reconfiguration [20]. An increase in power output has been observed under partial shading conditions [21] by altering interconnections [22]. Different shading patterns [23] have been analyzed for investigating the performance of TCT, HC and SP interconnection topology under shading conditions [24]. An analysis of shading faults in PV arrays with respect to different interconnections [25] in the literature is presented in Table 1. Further research is needed to investigate the effect of other electrical faults like short circuit, open circuit and their impact under shading on different interconnections of PV array and PV technology [17].

**Table 1.** Comparative analysis of shading condition in PV with respect to interconnections.

Condition	Interconnections	Increase in Power Generation	Ref.
Partial shading	Series (S)	11–17% power increase in TCT than other	[21]
	Series-Parallel (SP)	4% power increase in TCT	[22]
	Honey-Comb (HC)	10% power increase in HC than SP	[23]
	Total-Cross-Tied (TCT)	10–20% power increase in TCT than other	[24]
		5–10% power increase in TCT than SP	[25]

In this research paper, a unified approach is adopted for comparative analysis of faults such as open circuit, short circuit and severe shading in different interconnections of PV arrays including SP, HC and TCT interconnection. A special case of multiple faults in PV array under non-uniform shading is also investigated to analyze the combined impact of short circuit and open circuit fault under severe shading on P-V characteristics. It aims at enhancing power generation through optimizing the maximum power point (MPP) of the P-V characteristic curve and improving the performance of the power grid during severe faults. Therefore, monocrystalline and thin film (amorphous silicon) PV materials are considered for a more detailed analysis of faults. Thin-film PV technology optimizes the performance of PV systems in all fault scenarios. The utilization of suitable interconnection improves the obtained results which have been compared in terms of P-V curves. The main contributions of this paper can be listed as follows:

- (1). An increase in power generation is achieved through the utilization of suitable PV interconnection and PV material under different fault scenarios; it should be noted that in the literature, faults impact on PV arrangement and PV material is not studied thoroughly. Only the impact of shading and high temperature on PV arrangements is studied in the literature. The performance of

thin-film PV under short circuit and open circuit faults is also investigated in this paper, which has not been done so far.

- (2). A special case of multiple faults under non-uniform shading is also investigated in this paper for an analysis of the combined impact of all developed faults in PV array under severe shading conditions. The impact of all faults on the power grid is also investigated. It is found that the utilization of suitable PV interconnections and PV material also helps minimize the fault impact on power grids, which has also not been thoroughly studied in the literature.
  - i. The rest of this article is organized as follows: Classification of PV array faults based on location is presented in Section 2. The system model and interconnection schemes of PV array under different fault scenarios are explained in Section 3. Simulation results of PV array and its impact on power grids are presented in Section 4. A comparison and discussion of results are included in Section 5. Distinctive features are presented in Section 6, and a conclusion is drawn based on results in Section 7.

## 2. Classification of PV Faults

Typical faults in the PV system are given in Table 2. and are classified on the basis of type and location [1]. PV module mismatch faults due to partial shading and wiring losses due to short circuits within a PV module string and among different PV strings, line-to-line, and line-to-ground faults are common faults in PV systems. These faults may result in low power generation and can lead to permanent damage of a PV system.

**Table 2.** Classification of PV faults.

Part.	Fault type	Fault Condition	Description
D.C side	Shading fault/ PV module mismatch fault	Non-uniform shading [26,27]	Obstruction of trees and building causes partial shading on PV panels
		Uniform shading [9]	Different value of irradiance throughout the day minimizes power generation
	Short-circuit fault	Line-to-line fault [28] Line-to-ground [6]	Short circuit between PV modules Short circuit with ground
	Open-circuit fault	Disconnection of PV modules [10]	Disconnection between PV modules develops open circuit fault
A.C side	Degradation fault MPPT faults	Cracks of PV cells [14] Charging issue [29]	Defects of PV cell degrade performance Charging problem in controller
	Inverter faults	Problems in inverter [30]	Problems in any component of inverter leads to failure of inverter

## 3. System Model

In this section, a PV array model which is under study is presented for evaluation of the performance of a PV system under various fault scenarios. The system model is described briefly in the flow chart of the proposed methodology which mainly contains modeling of PV arrays and interconnection schemes of PV arrays under various fault scenarios. Mathematical modeling is also presented before a description of the proposed procedure for understanding its non-linear characteristic equations and the impact of faults on parameters of the PV model.

### 3.1. Mathematical Modeling

The equivalent circuit of a PV cell [31] is shown in Figure 1 in which the PV cell is represented as a current source in parallel to a diode. The photocurrent is represented by  $I_{ph}$  and shunt resistance is represented by  $R_{sh}$ . Both five parameters and seven parameters of single and double diode respectively can be used for analysis of electrical behavior of PV cells. The five parameter model [32] is considered in this research due to its higher accuracy for fault analysis and faster convergence of numerical methods than the seven parameter model.

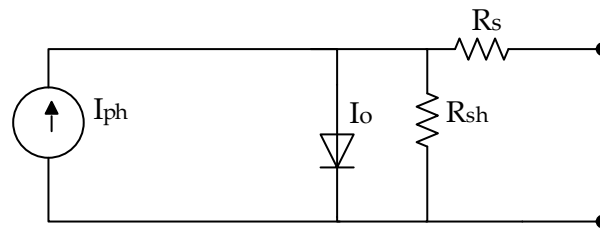


**Figure 1.** The equivalent circuit of PV cell.

The shunt resistance ‘Rsh’ denotes the flow of leakage current whereas ‘R<sub>s</sub>’ shows series resistance. The photocurrent of the PV module  $I_{ph}$  or  $I_L$  is a light-generated current and calculated using Equation (1).

$$I_{ph} = [I_{sc} + k_i(T - T_r)]G \quad (1)$$

where  $I_{sc}$  denotes short-circuit current in Amperes,  $k_i$  is the coefficient of  $I_{sc}$ ,  $T$  is the working temperature,  $T_r$  is the reference temperature i.e., 25 °C, and  $G$  is the solar irradiance of 1000 W/m<sup>2</sup>. Reverse saturation current is measured using Equation (2).

$$I_{rs} = \frac{I_{sc}}{\exp\left(\frac{qV_{oc}}{N_s k n T}\right) - 1} \quad (2)$$

where, the ‘ $q$ ’ charge of the electron is  $1.6 \times 10^{-19}$  C, ‘ $n$ ’ is the ideality factor of a diode,  $N_s$  is the number of series-connected cells,  $V_{oc}$  is open-circuit voltage, and ‘ $k$ ’ is Boltzmann’s constant which is equal to  $1.3805 \times 10^{-23}$  JK<sup>-1</sup>.  $E_{go}$  is the energy bandgap of the semiconductor. Saturation current is denoted by  $I_o$  and found using Equation (3)

$$I_o = I_{rs} \left[ \frac{T}{T_r} \right]^3 \exp \left[ \frac{q \times E_{go}}{nk} \left( \frac{1}{T} - \frac{1}{T_r} \right) \right] \quad (3)$$

The output current and voltage is represented by ‘ $I$ ’ and ‘ $V$ ’ respectively as found in Equation (4).

$$I = N_p \times I_{ph} - N_p \times I_o \times \left[ \exp \left( \frac{\frac{V}{N_s} + \frac{I \times R_s}{N_p}}{n \times V_t} \right) - 1 \right] - I_{sh} \quad (4)$$

The thermal voltage of the diode is represented as  $V_t$ , and shunt current  $I_{sh}$  is found by Equation (5).

$$I_{sh} = \frac{V \times \frac{N_p}{N_s} + I \times R_s}{R_{sh}} \quad (5)$$

$V_{oc}$  and  $I_{sc}$  are open-circuit voltage and short-circuit current respectively and can be calculated mathematically [8] as follows in Equations (6) and (7) [33].

$$I_{sc} = N_p \left( \frac{I_{STC}}{1000} \times G_R + k_I(T - T_{STC}) \right) \quad (6)$$

$$V_{oc} = N_s (V_{STC} + k_v(T - T_{STC}) + V_t \times \ln \left( \frac{I_{sc}}{I_{STC}} \right)) \quad (7)$$

Whereas,  $N_s$  and  $N_p$  are the number of series and parallel connected PV cells, respectively,  $I_{STC}$  is the short-circuit current at STC with irradiation = 1000 W/m<sup>2</sup> and  $T_{STC} = 25$  °C, whereas  $V_{STC}$  is the open-circuit voltage of the module at STC.  $G_R$  is received irradiance in W/m<sup>2</sup>.  $k_v$  is the temperature coefficient of open-circuit voltage.

### 3.1.1. Current and Voltage as Indicator of Fault

Any fault occurrence in the PV array affects the value of output voltage and output current due to their dependency on irradiance and temperature coefficients.  $I_{mp}$  and  $V_{mp}$  are the maximum current and maximum voltage, respectively, which can be calculated mathematically in Equations (8) and (9) as follows:

$$I_{mp} = N_p \left( \frac{I_{STC}}{1000} \times G_R + k_I (T - T_{STC}) \right) \quad (8)$$

$$V_{mp} = N_s \left( V_t \times \ln \left( 1 + \frac{I_{sc} - I_m}{I_{sc}} \left( e^{\frac{V_{oc}}{N_s V_t}} - 1 \right) \right) - \frac{I_m}{N_p} \times R_s \right) \quad (9)$$

The proposed procedure verifies the variation in physical quantities  $I_{mp}$  and  $V_{mp}$  after fault occurrence through P-V curve analysis.

### 3.1.2. Algorithm for P-V Curve Analysis

Many interconnected PV cells are packaged in the same PV modules and have the same irradiance value. Therefore, modeling and simulation of PV modules is a key step for the analysis of the P-V curve under normal and fault conditions. PV modules take values of received irradiance and temperature as input parameters to find a solution for current 'I' for sending this value to the controlled current source. The P-V curve is plotted after sending measured values of dc voltage and dc current through output parameters of PV modules including  $I_{sc}$ ,  $V_{oc}$ ,  $V_{mp}$ , and  $I_{mp}$  as given in the algorithm for the P-V curve in Figure 2.

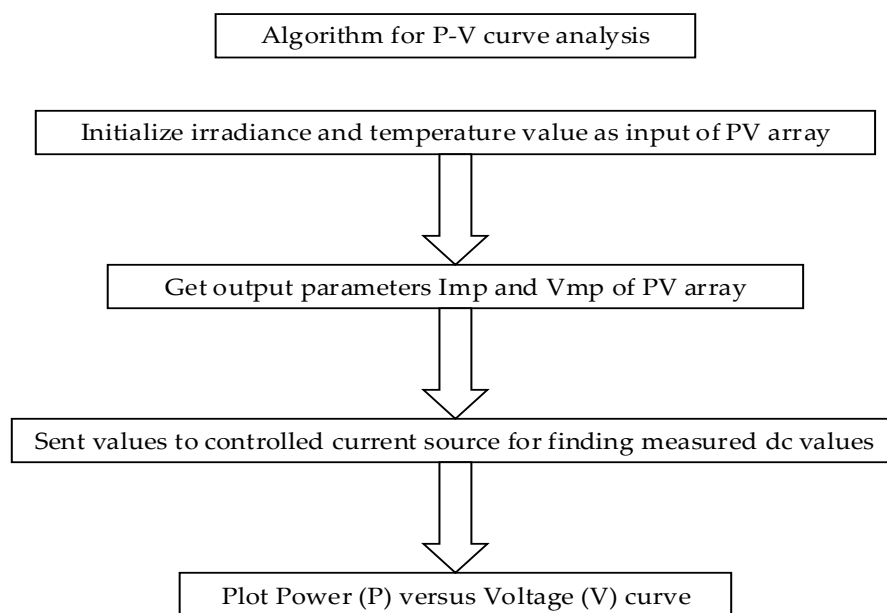


**Figure 2.** Algorithm for P-V curve analysis.

### 3.2. Flow Chart of Proposed Methodology

The flow chart of the proposed methodology is given in Figure 3. A Simulink model of a  $6 \times 6$  PV array under electrical faults including module disconnection, short circuit, and module mismatch faults is developed to study the performance of faulted PV array. A special case of multiple faults is also analyzed to study the impact of short-circuit and open-circuit faults under low irradiance conditions on peak power. All faults are thoroughly analyzed on crystalline and thin-film PV technology in all adopted interconnections. The impact of the proposed procedure on performance of a power grid is also analyzed for performance optimization of the PV system.

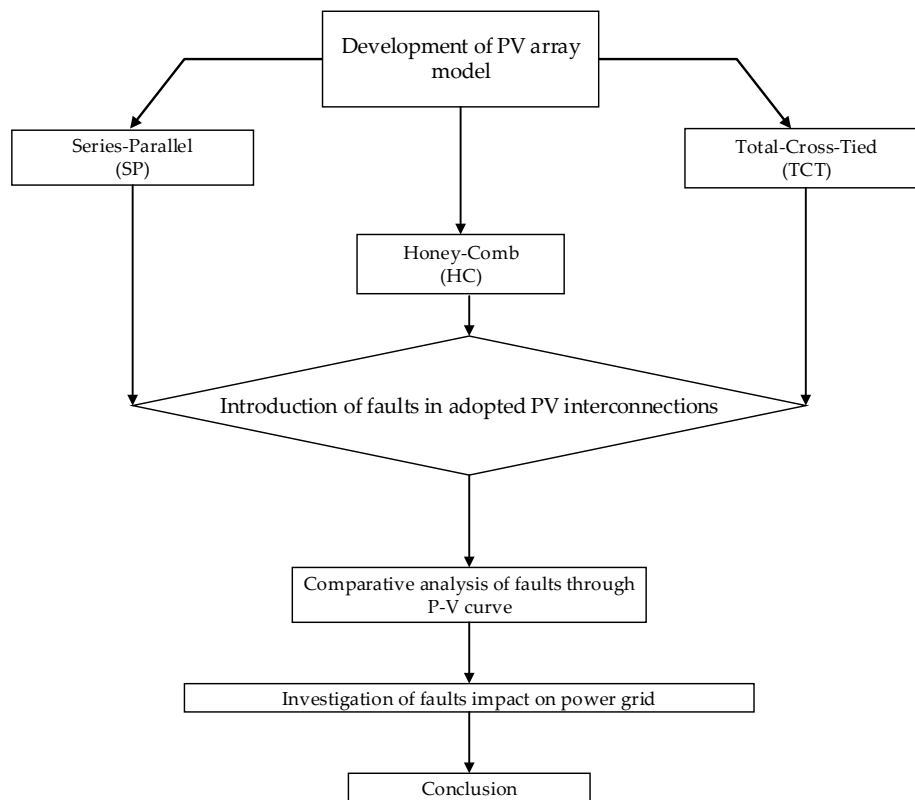


Figure 3. Flow chart of proposed methodology.

### 3.2.1. Modeling of PV Array

A 6 × 6 PV array is modeled in MATLAB with a single PV module of 150 Watts. The specifications of the considered PV module are given in Table 3.

Table 3. Parameters of the considered PV modules.

Open-Circuit Voltage $V_{oc}$ (V)	Short-Circuit Current $I_{sc}$ (A)	Max. Power Output $P_{max}$ (W)	Max. Open-Circuit Voltage $V_{mp}$ (V)	Max. short-Circuit Current $I_{mp}$ (A)
43.2	4.86	Monocrystalline type of PV module 150	35.2	4.26
40.5	6.35	Thin-film (a-Si) type of PV module 150	30	5
Light generated Current $I_L$ (A)	Diode saturation current $I_o$ (A)	Diode ideality factor $n$	Shunt resistance $R_{sh}$ ( $\Omega$ )	Series Resistance $R_s$ ( $\Omega$ )
4.89	$6.95 \times 10^{-11}$	Monocrystalline type of PV module 0.94	89.33	0.678
6.652	$1.40 \times 10^{-10}$	Thin-film (a-Si) type of PV module 2.589	25.79	1.1184

### 3.2.2. Interconnection Schemes of PV Array

There are three configurations which are designed for the analysis of fault impact on PV array including SP in which PV modules are interconnected in series and parallel, HC in which PV modules are interconnected with more interconnections than series-parallel interconnections in H patterns, and TCT interconnection in which all modules are closely tied together with more interconnections than SP and HC interconnections, as shown in Figure 4.

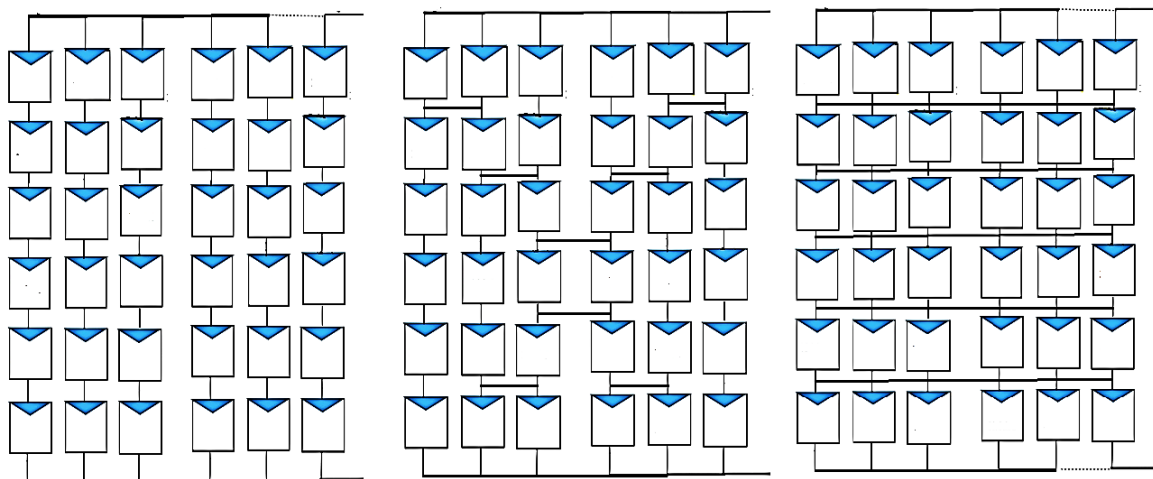


Figure 4. SP interconnection (Left), HC interconnection (Middle), TCT interconnection (Right).

### 3.2.3. Introduced Faults in PV Array

The following developed cases of faults are analyzed in adopted configurations of PV arrays as shown in Figure 5. All fault scenarios are analyzed in monocrystalline and thin-film types of PV material. The bypass diodes are connected with PV modules for protection from shading to shunt the current around them under shading condition. These diodes act as reverse bias in the normal operation of PV modules. The blocking diodes are connected with the PV modules to prevent the current flowing back into them.

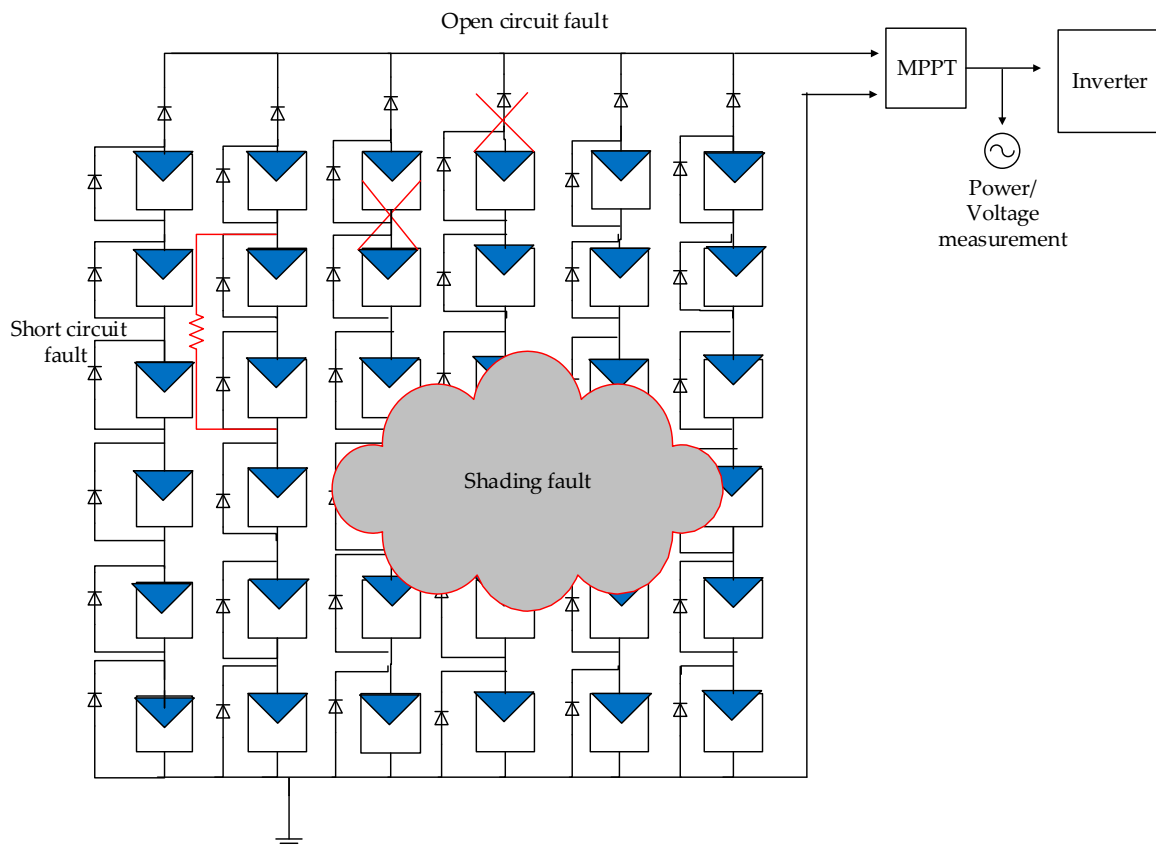


Figure 5. Introduced fault scenarios in PV array.

**Open-circuit fault in the PV array (F1):** Unintentional disconnection of PV module develops an open-circuit fault in the PV array. This Open-circuit fault is simulated by the disconnection of PV modules in the third and fourth PV string in this research. The impact of the fault is analyzed in the next section.

**Short-circuit fault in the PV array (F2):** An unintentional short circuit in a PV string can be referred to as line-to-line fault. A short-circuit fault is developed between PV modules in the second PV string in this fault scenario.

**Non-uniform shading fault (F3):** Non-uniform insulation develops a PV module mismatch fault. In this study, a complicated partial shading pattern is observed in this study for mismatch fault as shown in Table 4. 'n' represents PV modules connected in series, and 'm' represents parallel-connected strings of the PV module. Different values of irradiance are received by each interconnected PV module. For example:  $n=1, m=1$  i.e., the first PV module in the first PV string received  $1000 \text{ W/m}^2$  irradiance.

**Table 4.** Non-uniform shading pattern of PV array for F3 and F4.

n×m	m = 1	m = 2	m = 3	m = 4	m = 5	m = 6
	W/m <sup>2</sup>					
n = 1	1000	500	1000	1000	500	500
n = 2	1000	500	1000	1000	500	500
n = 3	1000	500	1000	1000	500	500
n = 4	400	700	400	400	700	700
n = 5	400	700	400	400	700	700
n = 6	400	700	400	400	700	700

**Multiple faults under non-uniform irradiance (F4):** A special case of multiple faults including short-circuit and open-circuit fault in PV array under non-uniform shading is introduced in this scenario for the analysis of the combined impact of faults on interconnections. The same non-uniform shading pattern is analyzed as observed in F3 in this case. This is a special case of faults and this situation can be developed in real life when faults occur during the day to night transitions.

Simulation results of all developed faults are presented in the next section.

#### 4. Simulations

In this section, simulation results of the proposed methodology are presented. The obtained results are compared in terms of the P-V curve, and the impact of all fault scenarios on the power grid is also investigated for a detailed comparative analysis of faults.

##### 4.1. Comparative Analysis of P-V curve

P-V curve is analyzed for comparative analysis of faults in all adopted PV configurations with respect to power generation. Firstly, fault-free operation is analyzed for the comparison of faults' impact on output parameters of the PV model. The parameters of the PV model in fault-free operation are given in Table 5.

**Table 5.** Parameters of the PV model in fault-free operation.

Max. Power Output $P_{\max}$ (kw)	Max. Open-Circuit Voltage $V_{mp}$ (v)	Max. Short-Circuit Current $I_{mp}$ (a)
5.4	Monocrystalline type 211.2	25.56
5.4	Thin-film (a-Si) type 180	30

The total output power is approximately 5.2 kWatts in standard testing conditions (STC) of 1000 W/m<sup>2</sup> irradiance and 25 °C temperature in fault-free operation as shown in Figure 6.

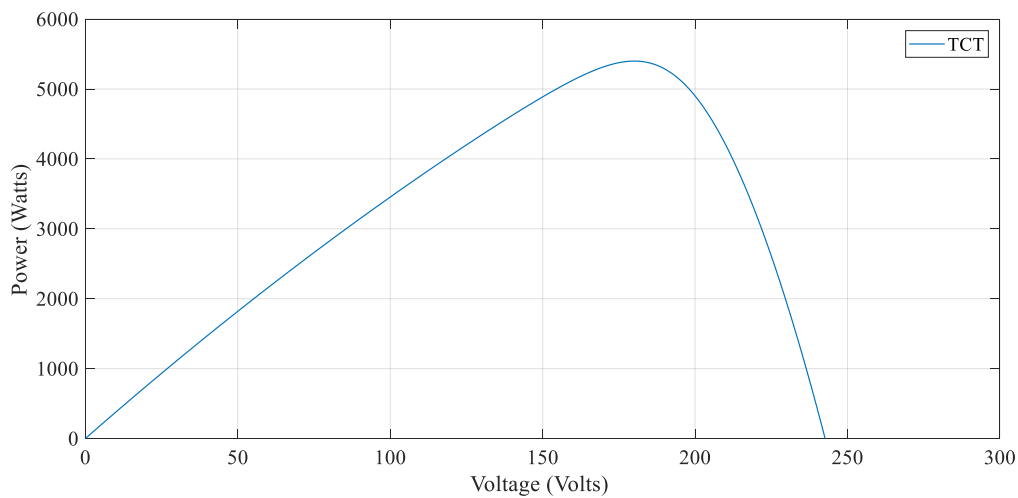


Figure 6. P-V curve for 6 × 6 PV array under normal conditions (STC).

Open-circuit fault (F1) reduces peak power from 5 kW to approximately 4.39 kW and 4.44 kW in the SP and HC interconnection of monocrystalline PV array, respectively, as shown in Table 6. The interconnection scheme of TCT optimizes peak power from 4.39 kW in simple SP interconnection to 4.9 kW. Thin-film PV technology performs better than monocrystalline through the optimization of MPP in all adopted interconnections. The increase in MPP from 4.8 kW to 4.94 kW in TCT, 4.5 kW to 4.66 kW in HC, and 4.39 kW to 4.53 kW in SP is achieved with minimization of multiple MPP’s in the P-V curve as shown in Figures 7 and 8.

Table 6. Parameters of the PV model during open-circuit fault (F1).

Type of Topology	Max. Power Output $P_{max}$ (kW)	Max. Open-circuit Voltage $V_{mp}$ (V)	Max. Short-Circuit Current $I_{mp}$ (A)
Monocrystalline type of PV module			
TCT	4.72	210.2	22.4
HC	4.44	209.4	21.2
SP	4.39	209.3	21.0
Thin-film (a-Si) type of PV module			
TCT	4.91	179	27.5
HC	4.64	178.5	26.1
SP	4.53	178.2	25.9

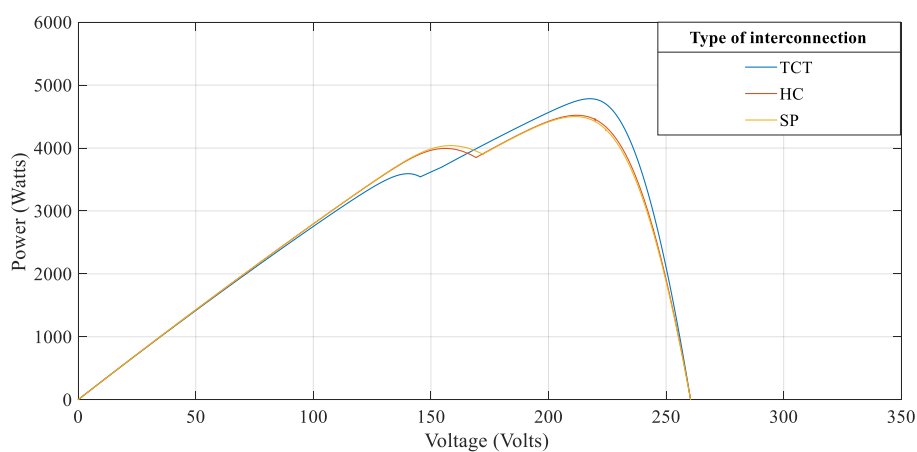


Figure 7. P-V curve for open-circuit fault ‘F1’ (monocrystalline PV).

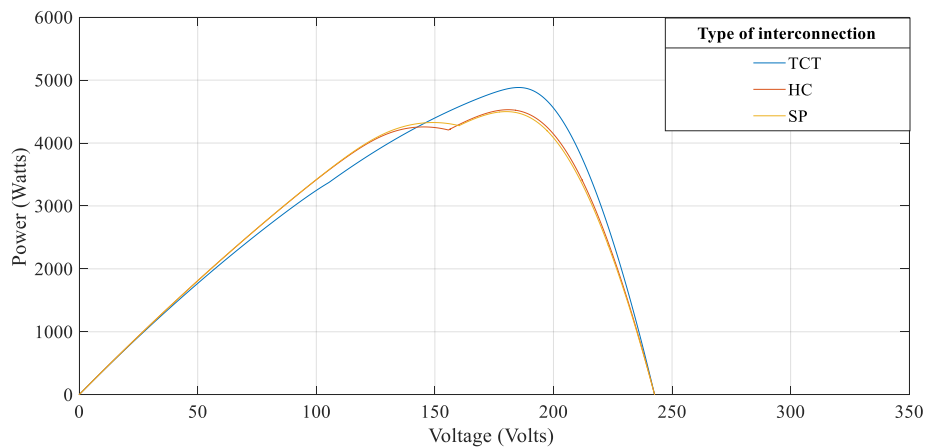


Figure 8. P-V curve for open-circuit fault 'F1' (thin-film PV).

P-V curves in Figures 7 and 8 show a comparative analysis of open-circuit fault (F1) in monocrystalline and thin-film PV respectively. A sudden decrease in peak power is due to a sudden decrease in current which is shown in the P-V curve of Figure 7

The parameters for short circuit fault (F2) are shown in Table 7 for the comparative analysis of short circuit fault (F2) in monocrystalline and thin-film PV, respectively. Peak power increases from 3.06kW to 3.36kW in SP, 3.01kW to 3.29kW in HC, and 2.6kW to 2.82kW in TCT interconnection.

Table 7. Parameters of PV model for short-circuit fault (F2).

Type of Topology	Max. Power Output $P_{max}$ (kW)	Max. Open Circuit Voltage $V_{mp}$ (V)	Max. Short Circuit Current $I_{mp}$ (A)
Monocrystalline type of PV module			
TCT	2.6	109	25.1
HC	3.0	118.5	25.57
SP	3.06	118.8	25.58
Thin-film (a-Si) type of PV module			
TCT	2.82	94.2	29.7
HC	3.29	107.7	30.5
SP	3.36	108.4	30.98

P-V curves in Figures 9 and 10 show a comparative analysis of short-circuit fault (F2) in monocrystalline and thin-film PV respectively. The MPP gets reduced due to the occurrence of short-circuit fault as shown in Figures 9 and 10.

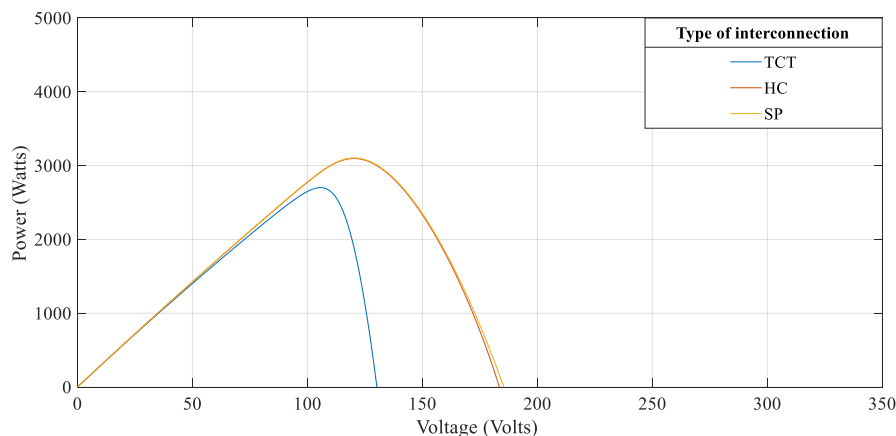


Figure 9. P-V curve for short circuit fault 'F2' (monocrystalline PV).

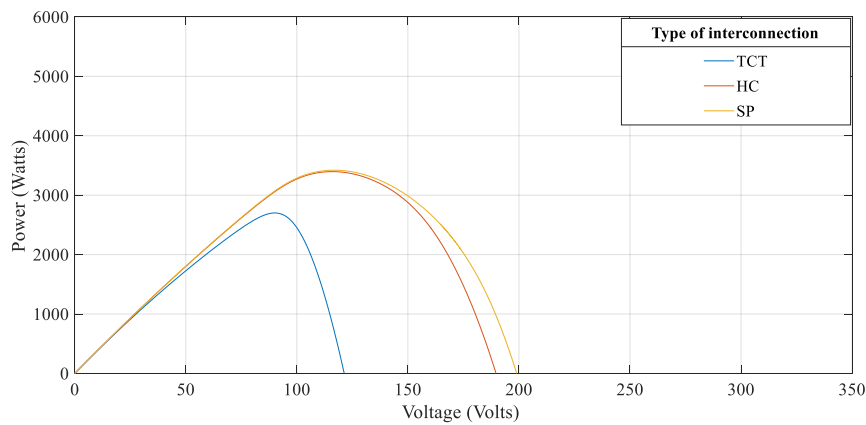


Figure 10. P-V curve for short circuit fault 'F2' (thin-film PV).

Short circuit fault reduces power from 5 kW to approximately 3.06 kW and 3 kW in SP and HC interconnections. TCT interconnection reduces MPP as compared to SP and decreases peak power from 3.15 kW to 2.6 kW. The adoption of TCT and HC interconnection fails to increase power generation during short-circuit fault. Thin-film PV technology optimizes the performance of all adopted interconnections.

Severe non-uniform shading fault (F3) reduces peak power from 5 kW to approximately 2.59 kW and 2.63 kW in SP and HC configurations, respectively, as shown in Table 8.

Table 8. Parameters of the PV model for non-uniform shading (F3).

Type of Topology	Max. Power Output $P_{max}$ (kw)	Max. Open-circuit Voltage $V_{mp}$ (v)	Max. Short-Circuit Current $I_{mp}$ (a)
Monocrystalline type of PV module			
TCT	2.98	221	13.481
HC	2.63	207.9	12.7
SP	2.57	205.7	12.5
Thin-film (a-Si) type of PV module			
TCT	3.19	201	15.8
HC	2.9	194.2	14.93
SP	2.77	187.1	14.8

The reduction in peak power and appearance of multiple MPPs in the P-V curve is due to the sudden decrease in current values. TCT configuration minimizes multiple power peaks and increases power from 2.57kW in SP to 2.98kW. TCT configuration optimizes MPP with the minimization of multiple peaks as shown in Figures 11 and 12

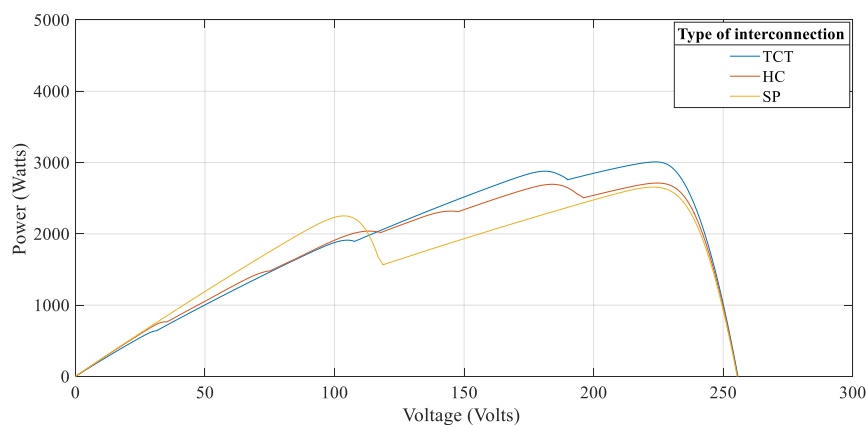


Figure 11. P-V curve for non-uniform shading 'F3' (monocrystalline PV).

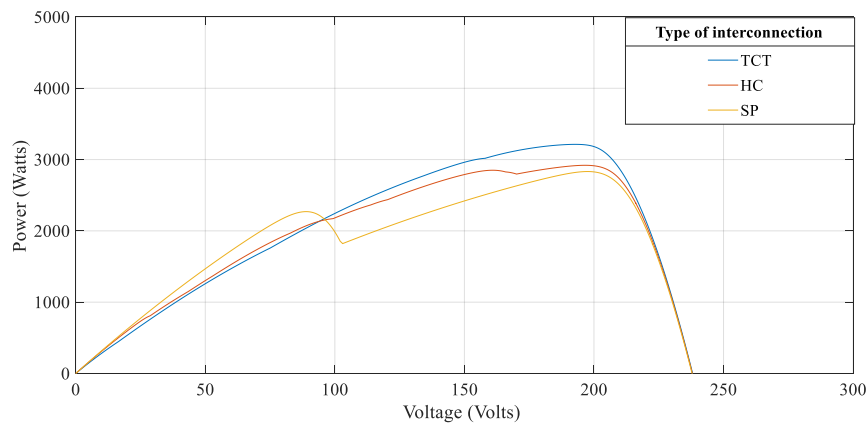


Figure 12. P-V curve for non-uniform shading ‘F3’ (thin-film PV).

Thin-film PV performs much better than monocrystalline PV in severe shading conditions and increases peak power from 2.57 kW to 2.77 kW in SP, 2.63 kW to 2.9 kW in HC, and 2.98 kW to 3.19 kW in TCT interconnection. The utilization of thin-film technology optimizes the P-V curve and multiple MPP’s almost diminish in TCT configuration.

Multiple faults during severe non-uniform shading fault (F4) reduce peak power from 5 kW to approximately 1.94 kW and 2.1 kW in SP and HC configuration, respectively, as shown in Table 9.

Table 9. Parameters of the PV model for multiple faults (F4).

Type of Topology	Max. Power Output $P_{max}$ (kw)	Max. Open-circuit Voltage $V_{mp}$ (v)	Max. Short-Circuit Current $I_{mp}$ (a)
Monocrystalline type of PV module			
TCT	1.89	150	12.6
HC	2.10	160	13.1
SP	1.94	156.4	12.4
Thin-film (a-Si) type of PV module			
TCT	2.0	133.3	15
HC	2.5	147.7	17
SP	2.31	144.3	16

The reduction in peak power and appearance of multiple MPPs in the P-V curve is due to a sudden decrease in current values. HC configuration performs better than other interconnections under multiple faults including short circuit and open circuit with severe shading and minimizes multiple power peaks as shown in Figures 13 and 14.

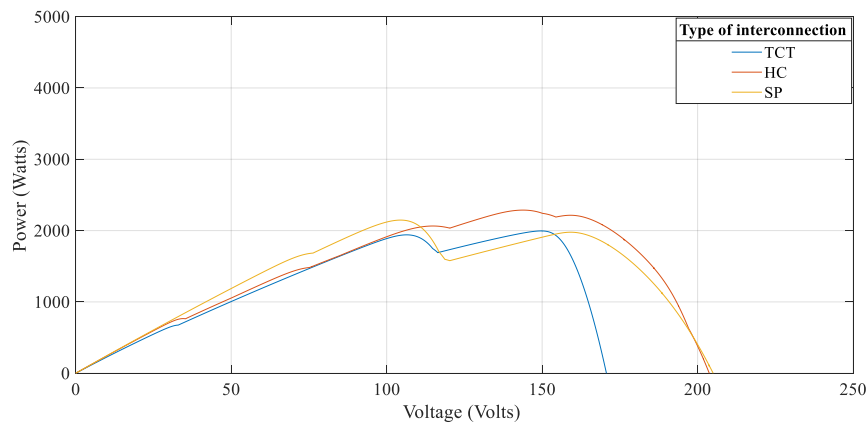
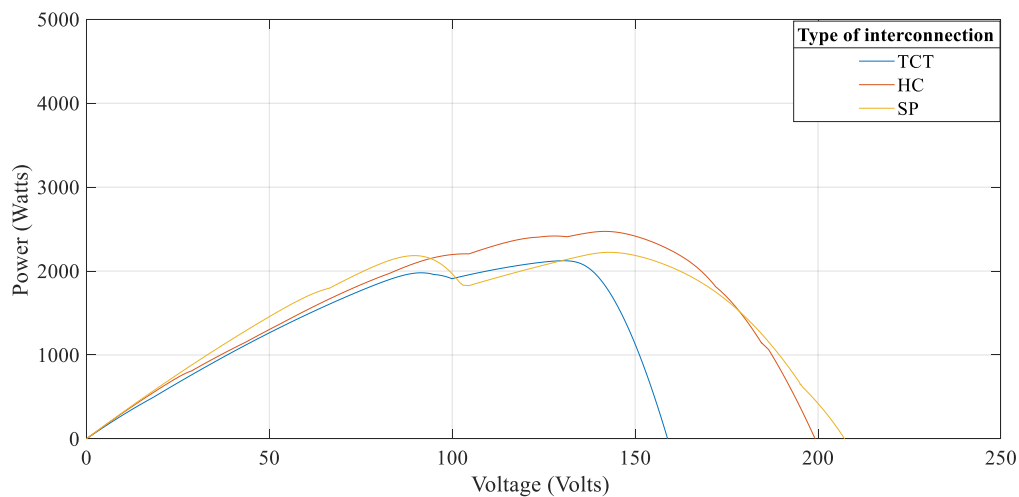


Figure 13. P-V curve for multiple faults ‘F4’ (monocrystalline PV).



**Figure 14.** P-V curve for multiple faults 'F4' (thin-film PV).

The increase in peak power from 1.89 kW in TCT to 2.1 kW in HC is observed with monocrystalline PV. Thin-film PV performs better than monocrystalline PV in the multiple fault scenario and increases peak power from 1.89 kW to 2.0 kW in TCT, 2.1 kW to 2.5 kW in HC, and 1.94 kW to 2.31 kW in SP interconnection. The utilization of thin-film technology optimizes the performance of the PV system in all fault scenarios.

Thin-film PV material performs better in all fault scenarios than monocrystalline PV material according to P-V curve analysis with respect to maximum power generation. The impact of thin film and monocrystalline PV in adopted interconnections on the performance of the power grid is also analyzed for a more detailed analysis of all fault scenarios.

#### 4.2. Impact of Faults on Power Grid

The  $6 \times 6$  PV array is integrated with a 25 kW grid via a DC-DC boost converter and inverter. The block diagram is given in Figure 15.

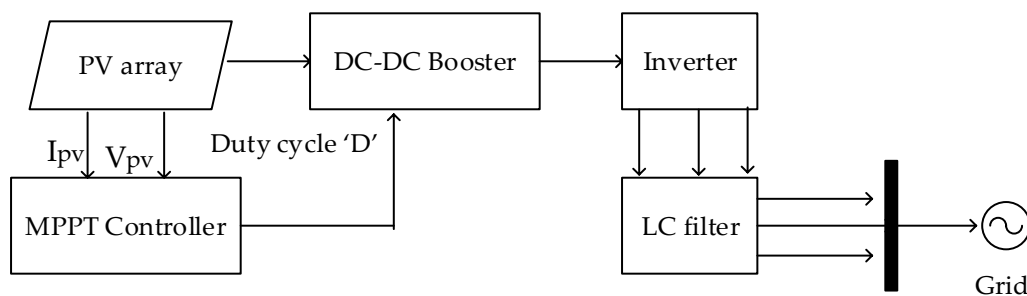


**Figure 15.** Block diagram of grid-connected PV system.

$V_{pv}$  and  $I_{pv}$  from the PV array are sent to the MPPT controller for tracking of MPP through controlling of the duty cycle. MPPT algorithm [19] tracks MPP by adjusting the operating voltage to track MPP. The voltage changes in the same direction if power increases, and voltage variation reverses its direction if power decreases. The algorithm of perturb and observe (P&O) [18] is easy to implement but the performance of this algorithm is not efficient enough to accurately track MPP during developed faults. The DC-DC boost converter is an important part of the PV system which boosts the voltage level after receiving control pulses 'D' through the MPPT algorithm. It consists of a capacitor, resistor, inductor, and high-speed switching device 'IGBT' with a diode. The circuit [34] is shown in Figure 16.

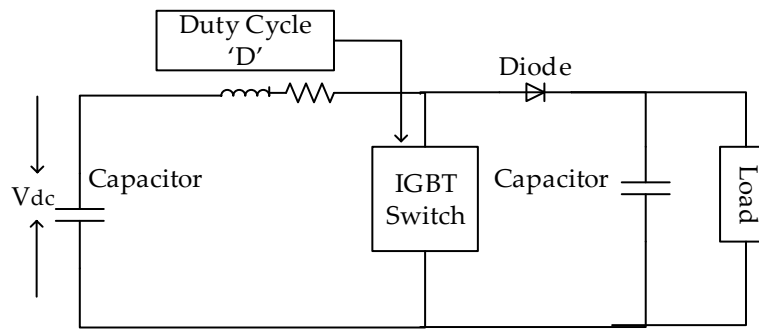


Figure 16. Circuit diagram of DC-DC boost converter.

A  $6 \times 6$  PV array is integrated with a 25 kW power grid for an analysis of the faults' impact on the power grid through observing the sequence of events on scope. Firstly, fault-free operation of the PV system is analyzed as shown in Figure 17. The duty cycle of the boost converter is fixed from the start to 3000 ms, and control pulses 'D' start changing after enabling MPPT. The MPPT is not enabled from the start which is evident from the disturbance, as shown in Figure 17, from the start to approximately 3000 ms. MPPT is enabled at approximately 3000ms and starts regulating MPP by adjusting the duty cycle. Approximately 5.2 kW MPP is tracked with a tracking time of approximately 3500 ms and continues to track MPP till the end under normal conditions, i.e.,  $1000 \text{ W/m}^2$  and  $25^\circ\text{C}$ . The same value of power will be delivered to the grid under unchanged operating conditions after enabling MPPT. So, only limited values are recorded till a range of 1500 ms.

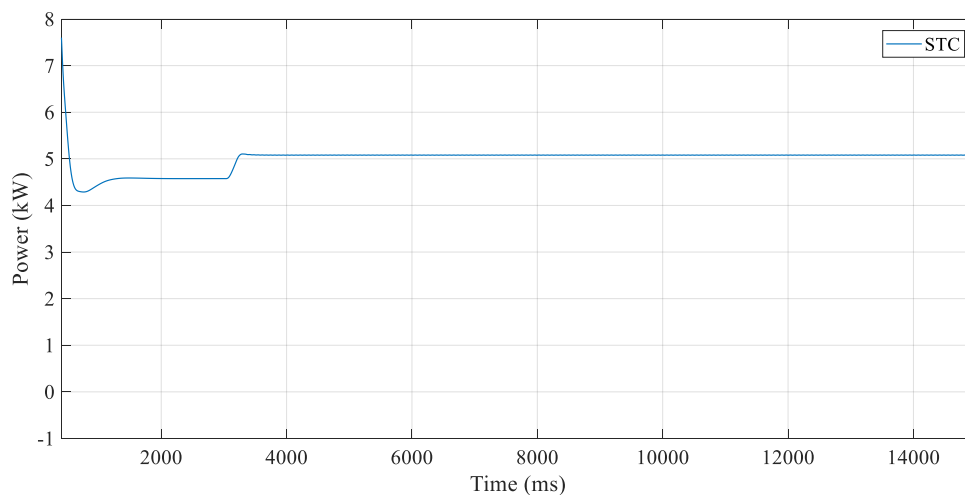
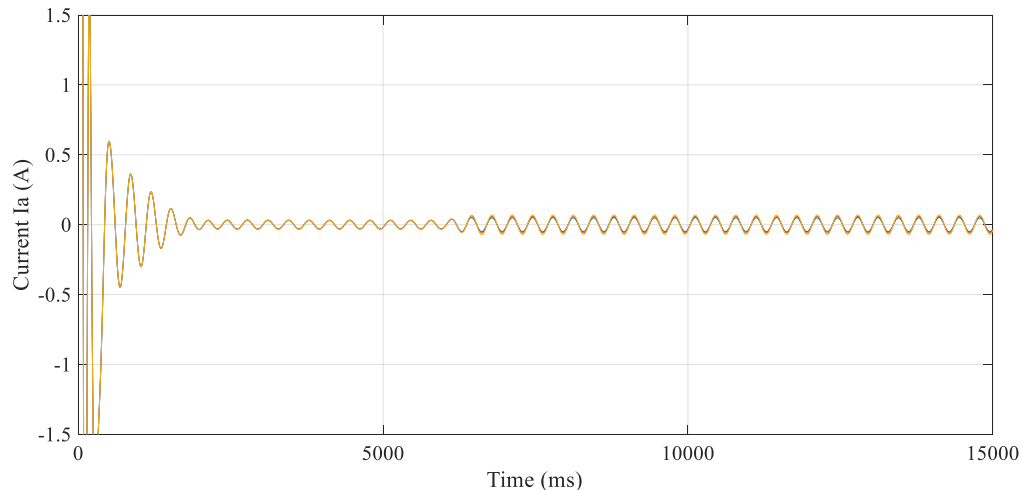


Figure 17. Power of the grid under normal condition.

This MPPT algorithm improves power generation but it is not efficient enough to track global MPP in a dynamic changing environment and tracks reduced power in all fault scenarios. Overcurrent protection devices (OCPD) are usually installed in PV systems to clear faults, but developed faults in the PV array cannot be cleared by OCPD due to operation of the MPPT algorithm which results in a small current. The decrease in grid current due to multiple faults in PV array under severe shading is shown in Figure 18. All faults developed in PV array and non-uniform shading decrease the current in the presence of MPPT and make the fault's impact less severe.

The impact of all faults is also investigated in all PV interconnection schemes integrated with a grid for the analysis of impact on the power grid. Faults are introduced from the start in all simulations. The grid power shows disturbance from the start but after MPPT is enabled at approximately 3000 ms and starts tracking reduced MPP less than 5.2 kW due to developed fault scenarios. Power generation reduces due to introduced faults and other losses such as inefficiency of MPPT and other transmission

losses. The severe impact of faults on the power output of the grid diminishes due to MPPT, but the algorithm makes early fault detection very difficult which can cause large fire accidents. The proposed methodology introduces SP, HC and TCT interconnections which change the MPP and improve power generation through an increase in MPP.



**Figure 18.** Reduction in current due to multiple faults in PV array under severe shading.

The arrangement of monocrystalline PV array in SP and HC interconnection during open-circuit fault (F1) reduces tracked MPP from 5.2 kW to 4.09 kW and 4.18 kW in SP and HC interconnection, respectively, after enabling MPPT at 3000 ms and continues to track the reduced MPP till the end as shown in Figure 19. TCT interconnection minimizes this power loss and increases tracked MPP from 4.09 kW to 4.5 kW. Thin-film PV further minimizes power loss by increasing tracked MPP from 4.5 kW to 4.8 kW in TCT interconnection as shown in Figure 20. The interconnection of SP and HC in thin-film type PV array increases tracked MPP to 4.14 kW and 4.23 kW, respectively, and increases power generation in comparison to monocrystalline PV.

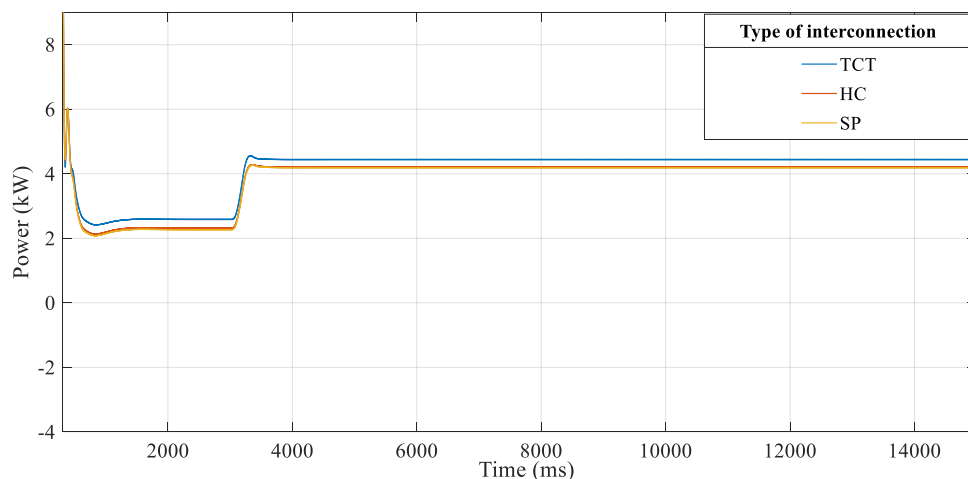


**Figure 19.** Impact of open-circuit fault 'F1' on power grid (monocrystalline PV).

Short circuit fault (F2) reduces tracked MPP from 5.2 kW to 2.27 kW and 2.51 kW in TCT and HC interconnection, respectively, after 3000 ms and continues to track the reduced MPP till the end. SP interconnection performs better than other interconnections and produces tracking power of a 2.62 kW in monocrystalline PV array, as shown in Figure 21. Thin-film PV optimizes the PV performance through increasing tracked MPP from 2.62 kW to 3.01 kW in SP, 2.51 kW to 2.8 kW in HC, and 2.275 kW

to 2.75 kW in TCT as shown in Figure 22. TCT interconnection cannot optimize performance in this fault case. Only power loss compensation through TCT interconnection can be achieved under those faults, which results in a sudden decrease of current due to more internal connections in TCT and more current flow in TCT than other interconnections as observed in open-circuit fault (F1) and shading conditions (F3).

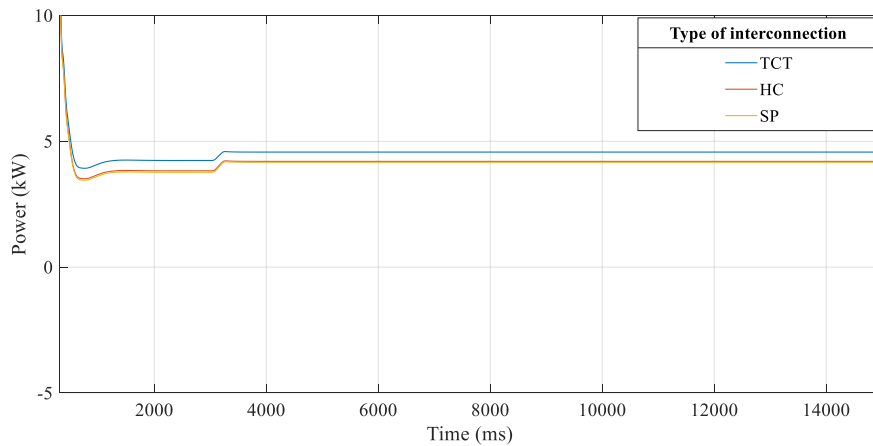


Figure 20. Impact of open-circuit fault 'F1' on power grid (thin-film PV).

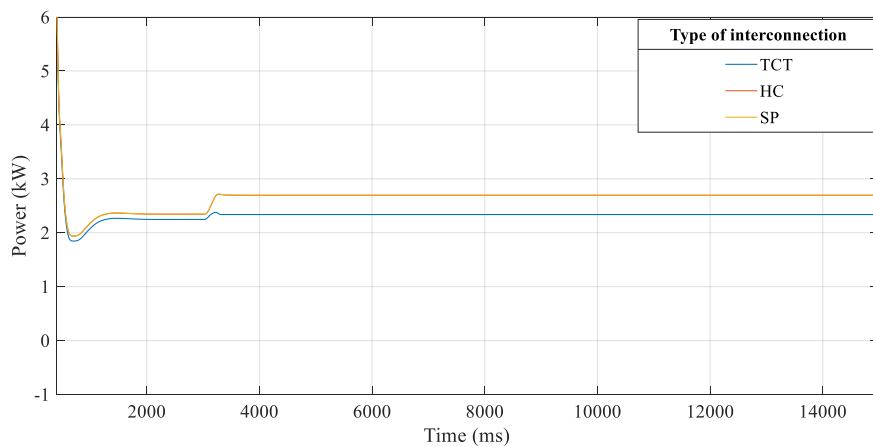


Figure 21. Impact of short-circuit fault 'F2' on power grid (monocrystalline PV).

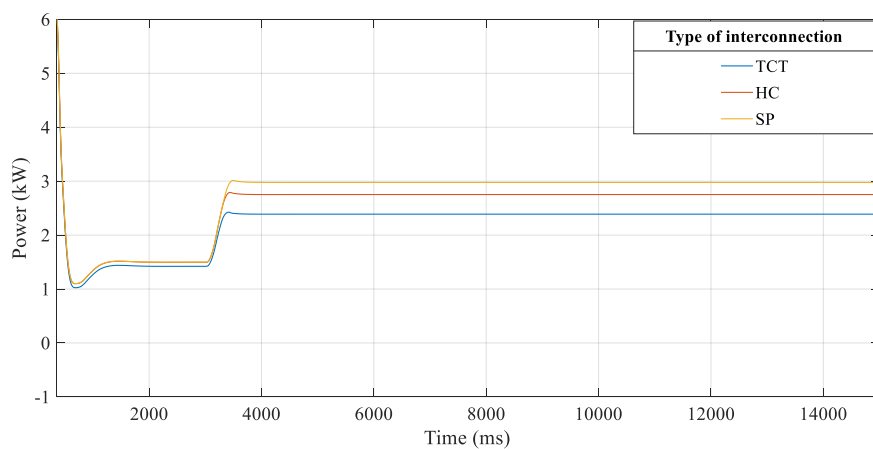
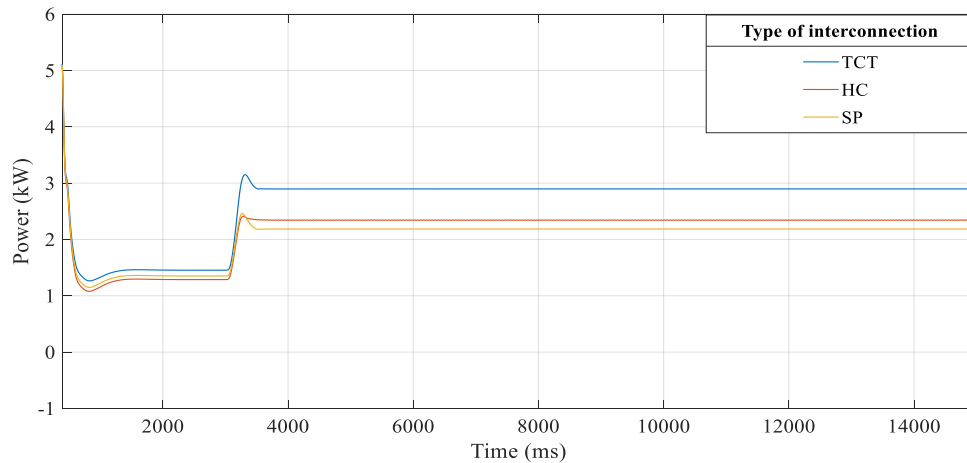
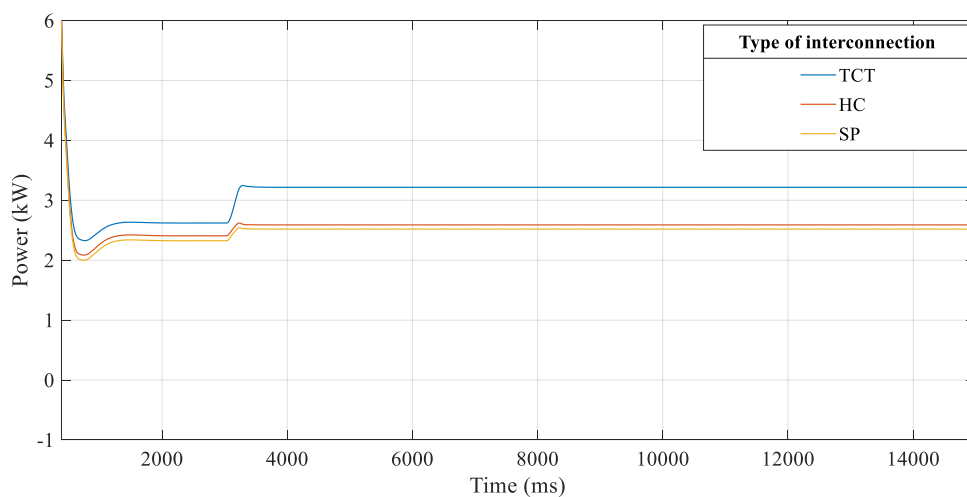


Figure 22. Impact of short-circuit fault 'F2' on power grid (thin-film PV).

Severe shading in mismatch fault 'F3' reduces tracked MPP from 5.2 kW to 2.8 kW, 2.19 kW and 2.1 kW in TCT, HC and SP, respectively, in monocrystalline PV as shown in Figure 23. TCT interconnection minimizes power loss in a grid-integrated PV system. Thin-film optimizes PV performance in shading fault and increases power from 2.8 kW to 3.2 kW, 2.19 kW to 2.55 kW, and 2.2 kW to 2.51 kW in TCT, HC and SP respectively as shown in Figure 24.



**Figure 23.** Impact of non-uniform shading fault 'F3' on power grid (monocrystalline PV).



**Figure 24.** Impact of non-uniform shading fault 'F3' on power grid (thin-film PV).

Multiple faults under severe non-uniform shading (F4) reduce tracked MPP from 5.2 kW to 1.4 kW, 1.8 kW and 1.62 kW in TCT, HC and SP, respectively, in monocrystalline PV as shown in Figure 25. HC interconnection optimizes the performance of the power grid by minimizing the losses of SP and TCT interconnection. Thin-film PV material increases tracked peak power from 1.4 kW to 1.71 kW, 1.8 kW to 2.01 kW and 1.6 kW to 1.74 kW in TCT, HC, and SP, respectively, as shown in Figure 26. HC performance is better due to the combined impact of all faults in this case.

Thin-film PV technology performs better than monocrystalline in all developed faults and optimizes the performance of the PV system through an increase in peak power as shown in Table 10.

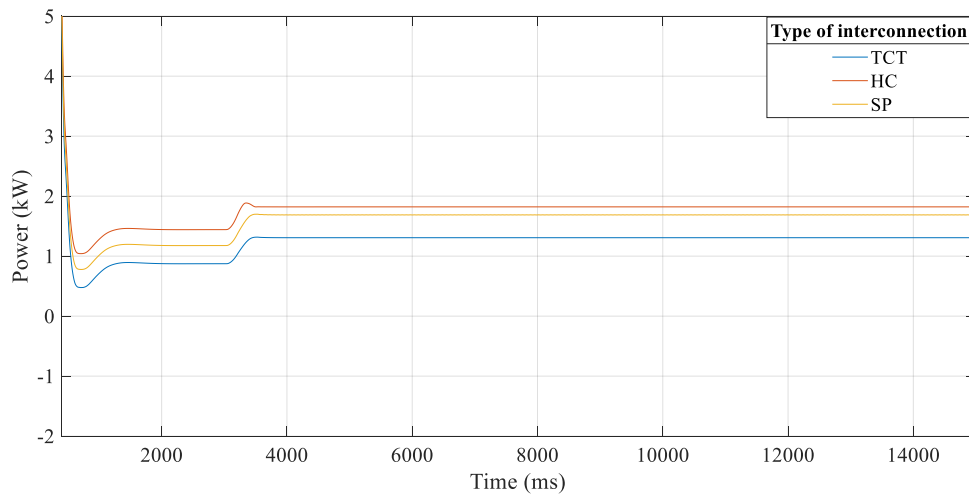


Figure 25. Impact of multiple faults 'F4' on power grid (monocrystalline PV).

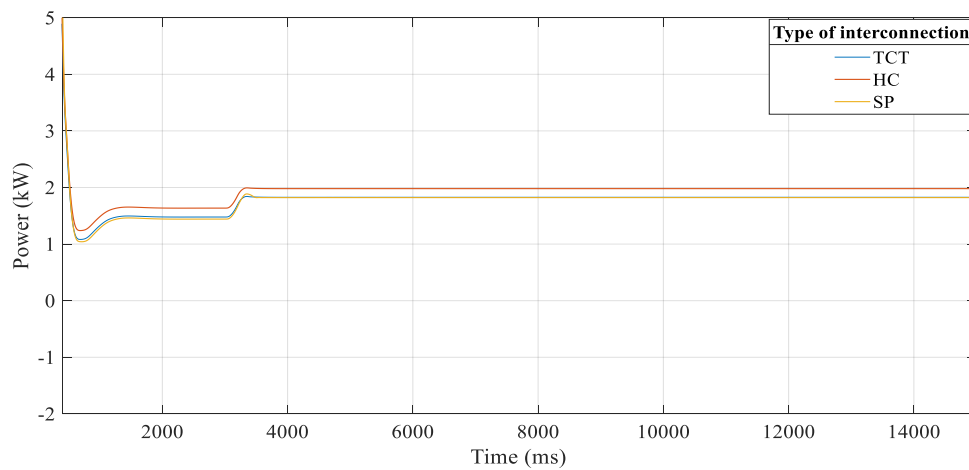


Figure 26. Impact of multiple faults 'F4' on the power grid (thin-film PV).

Table 10. Comparison of adopted interconnections in PV array.

Topology	$P_{max}$ in Fault Scenarios (kW)							
	Monocrystalline PV				Thin-Film (a-Si) PV			
	F1	F2	F3	F4	F1	F2	F3	F4
SP	4.39	3.06	2.57	1.94	4.53	3.36	2.75	2.31
HC	4.44	3.0	2.63	2.1	4.64	3.29	2.9	2.5
TCT	4.72	2.6	2.98	1.89	4.91	2.82	3.19	2.0
Grid-integrated PV system								
SP	4.09	2.62	2.4	1.60	4.14	3.01	2.6	1.74
HC	4.18	2.51	2.5	1.8	4.23	2.8	2.76	2.01
TCT	4.5	2.27	2.8	1.4	4.8	2.6	3.02	1.71

### 5. Discussion

In this section, the obtained results are compared and discussed in detail. An increase in power generation during all developed faults is calculated by comparing the MPP of designed interconnection, which produced reduced peak power, with the considered interconnection as shown in Equation (10), and a detailed comparison of results is given in Table 11.

$$P_{CI} = \text{Power of considered interconnection}$$

$P_{LI}$  = Power of designed interconnection which produced lowest peak power

$$\text{Increase in power} = \frac{P_{CI} - P_{LI}}{P_{LI}} \times 100 \quad (10)$$

**Table 11.** Comparative analysis of results as represented in Table 10.

Topology	Increase in $P_{max}$ (Monocrystalline PV)				Increase in $P_{max}$ (Thin-Film (a-Si) PV)			
	F1	F2	F3	F4	F1	F2	F3	F4
SP	0%	17%	0%	2.6%	0%	19.1%	0%	0.9%
	increase	increase	increase	increase	increase	increase	increase	increase
HC	1.1%	15.3%	2.3%	11%	2.4%	16%	5.4%	25%
	increase	increase	increase	increase	increase	increase	increase	increase
TCT	7.5%	0%	15.9%	0%	8.3%	0%	16%	0%
	increase	increase	increase	increase	increase	increase	increase	increase
<b>Grid-integrated PV system</b>								
SP	0%	15%	0%	14.5%	0%	15%	0%	15.5%
	increase	increase	increase	increase	increase	increase	increase	increase
HC	2.2%	10%	4.1%	28%	2.1%	7.6%	6.1%	17.7%
	increase	increase	increase	increase	increase	increase	increase	increase
TCT	10%	0%	14.2%	0%	15.9%	0%	16.1%	0%
	increase	increase	increase	increase	increase	increase	increase	increase

The obtained results are compared in all fault scenarios. The SP interconnection generates the least power output in open-circuit fault (F1). TCT increases maximum generated power output by 7.5% and 8.3% with monocrystalline and thin-film PV material respectively. A 1.1% increase in power is obtained by adopting HC in monocrystalline, and a 2.4% increase in thin-film PV in comparison to SP interconnection is obtained.

TCT interconnection produces less peak power in comparison to HC and SP under short-circuit fault (F2). An approximate 19% increase in generated peak power is obtained by adopting SP in short circuit fault (F2) with thin-film PV, and a 17% increase in power with monocrystalline PV in comparison to TCT interconnection is achieved. SP produces less power generation than other topologies in severe shading fault (F3). An approximate 2.3% increase in power by the adoption of HC with monocrystalline and 5% with thin-film PV is achieved. An approximate 15% increase in power generation by the adoption of TCT with monocrystalline and 16% with thin-film PV is achieved due to more internal connections and current flow. HC performed better than other configurations in the case of multiple faults under severe shading due to a better performance than SP in shading fault, open circuit fault and better performance than TCT in short circuit fault. The combined impact of all faults reduces the performance of both TCT and SP. So, HC performs better than others in this case.

In the comparative analysis of faults in grid-integrated PV systems, the interconnection of TCT increases MPP by 10% with monocrystalline and 15% with thin-film PV in open circuit fault (F1); a 2.2% increase in monocrystalline and 2.4% increase in thin-film is achieved in the HC interconnection scheme. SP increases MPP by 15.8% with thin film and 15% in monocrystalline under short-circuit fault (F2). A 10% and 7.6% increase in power is achieved by the adoption of HC with monocrystalline, and thin-film PV is achieved. A 14% increase by TCT under severe shading (F3) with thin film and 16% increase with monocrystalline by TCT in power generation is achieved. A 4% increase in MPP with monocrystalline and 6% increase with thin-film in HC is achieved in shading fault (F3). HC performs better than other interconnections in multiple faults under severe shading (F4) through an increase in MPP by 26% and 17% in monocrystalline and thin-film PV, respectively. The detailed comparison of increased power generated is shown in Table 11 for both monocrystalline and thin-film PV material.

Thin-film PV material performs better in all developed fault scenarios and shows more efficient performance than monocrystalline as shown in Table 12. The efficiency ( $\eta$ ) can be calculated by Equation (11) as given below:

$$\eta = \frac{P_{tf} - P_{mc}}{P_{\max}} \quad (11)$$

$P_{tf}$  = Maximum power achieved by thin-film PV

$P_{mc}$  = Maximum power achieved by monocrystalline PV

$P_{\max}$  = Maximum power achieved at *STC* i.e., 1000 W/m<sup>2</sup> and 25 °C

**Table 12.** Efficiency comparison of thin film with monocrystalline PV in fault scenarios (FS).

Topology	Efficiency of 6 × 6 PV Array				Efficiency of Grid-Connected 6 × 6 PV Array			
	F1	F2	F3	F4	F1	F2	F3	F4
SP	2.6%	5.6%	3.3%	6.9%	1%	7%	3.8%	2.6%
HC	4.5%	5.45%	5%	7.5%	1%	5.5%	4.8%	5.9%
TCT	3.4%	4.1%	3.9%	2.0%	5%	6%	4.3%	5.9%

Thin-film PV material maximizes power generation and shows higher efficiency than monocrystalline according to P-V curve analysis. Thin-film PV material also improves the performance of the power grid and achieves higher efficiency according to simulation results. Only the power generation of a defective cell is affected after the occurrence of a fault in thin-film PV material, but the functioning of other connected cells is not affected by the occurrence of a fault. The functioning of the whole PV module is affected through the development of a fault in one PV cell of monocrystalline. Thus, thin-film PV has higher power generation during fault conditions.

## 6. Distinctive Features of Proposed Methodology

- (1). This paper presents a detailed investigation of faults including non-uniform shading, open circuit and short circuit in different PV interconnections. A special case of multiple faults in PV array under non-uniform irradiance is also investigated to analyze their combined impact on utilized PV interconnections.
- (2). The impact of all faults on the power grid is also investigated for a detailed analysis of faults on a PV system.
- (3). An increase in power generation is achieved through the utilization of suitable PV interconnection and thin-film PV material under different fault scenarios; it should be noted that in the literature, faults impact on PV arrangement and PV material is not studied thoroughly. Only the impact of shading and high temperature is studied in the literature for PV arrangements and technology.
- (4). The performance of thin-film PV under short circuit and open circuit fault is also investigated in this paper. The performance of thin-film PV under all developed faults in PV array with the arrangement of TCT and HC has not been done before. The utilization of thin-film PV with TCT interconnection optimizes the system performance by an 8.3% and 16% power increase in P-V curve analysis and by 15.9% and 16.1% power increase in a grid-connected PV system under open circuit (F1) and severe shading fault (F3), respectively.
- (5). A special case of multiple faults under non-uniform shading is investigated in this paper for the comparison of PV technologies and interconnections. The combined impact of all developed faults in PV arrays is analyzed under severe shading conditions for a detailed comparative analysis which has not been done before. The utilization of thin-film PV with an HC interconnection optimizes the system performance by 11% and 25% power increases in P-V curve analysis and by 28% and 17% power increases in a grid-connected PV system during multiple faults under severe shading (F4), respectively.

- (6). The unified approach of utilizing both-thin film PV and monocrystalline PV technology in three different arrangements of PV including TCT, HC and SP for detailed comparative analysis of their impact on a power grid is a major contribution of this research.

## 7. Conclusions

In this research, a detailed comparative analysis of faults in different PV interconnection schemes including SP, HC, and TCT in terms of a P-V characteristic curve is presented. It is investigated that TCT can enhance power generation in open circuit and severe shading fault due to more internal connections in comparison to SP and HC where a sudden decrease in current develops multiple MPPs. HC interconnection performs better than other interconnections during the case of multiple faults under severe shading due to the combined impact of all faults. In addition, a comparison of monocrystalline and thin-film PV material with respect to power generation is also presented. The performance of thin-film technology has only been investigated under shading in the literature. The performance of thin-film PV under all developed electrical faults is investigated in this research. It is found that thin-film PV material achieves higher peak power than monocrystalline in all developed faults. Thus, the thin-film PV technology with suitable interconnection topology optimizes power generation during developed faults and also minimizes the severe impact on the power grid during all fault scenarios through an increase in tracked MPP.

Simulation results show the possibility of enhancing the power generation of PV arrays under severe faults through proposed methodology, and the investigation of various fault scenarios in different PV interconnections and materials can compensate power loss and improve the efficiency of the PV system. It would be useful to further investigate the impact of many different faults on different interconnection schemes and different PV technologies, and its practical implementation can also be considered as future work. The development of techniques and procedures is also needed to further improve the efficiency of thin-film PV technology for the safe and efficient operation of a PV system under developed faults.

**Author Contributions:** Conceptualization with implementation of the work, S.G.; Supervision and administration of the project, A.U.H.; Formal analysis, A.A.; investigation and formation of manuscript, I.U.K.; Critical review, M.J. All authors have read and agreed to the published version of the manuscript.

**Funding:** This research received no external funding.

**Conflicts of Interest:** The authors declare no conflict of interest.

## References

1. Sabbaghpur Arani, M.; Hejazi, M.A. The Comprehensive Study of Electrical Faults in PV Arrays. *J. Electr. Comput. Eng.* **2016**, *2016*, 8712960. [[CrossRef](#)]
2. Anderson, B.; Anderson, R. *Fundamentals of Semiconductor Devices*; McGraw-Hill: New York, NY, USA, 2004.
3. Lee, C.; Suh, J.; Choi, Y. Comparative Study on Module Connections to Minimize Degradation of Photovoltaic Systems due to Bird Droppings. *Int. J. Renew. Energy Res.* **2018**, *8*, 230–237.
4. Firth, S.K.; Lomas, K.J.; Rees, S.J. A simple model of PV system performance and its use in fault detection. *Sol. Energy* **2010**, *84*, 624–635. [[CrossRef](#)]
5. Falvo, M.C.; Capparella, S. Safety issues in PV systems: Design choices for a secure fault detection and for preventing fire risk. *Case Stud. Fire Saf.* **2015**, *3*, 1–16. [[CrossRef](#)]
6. Brooks, B. *The Ground Fault Protection Blind Spot: A Safety Concern for Large Photovoltaic Systems in the United States*; A solar ABCs White Paper; CA, USA, 2012.
7. Brooks, B. *The Bakersfield Fire*; ABC white paper; SOLAR PRO, feb2011: CA, USA, 2011.
8. Patel, H.; Agarwal, V. Matlab-based modeling to study the effects of partial shading on PV array characteristics. *IEEE Trans. Energy Convers.* **2008**, *23*, 302–310. [[CrossRef](#)]
9. Nguyen, D.D.; Lehman, B. Modeling and simulation of solar PV arrays under changing illumination conditions. In Proceedings of the 10th IEEE Workshop on Computers in Power Electronics (COMPEL'06), Troy, NY, USA, 16–19 July 2006; pp. 295–299.

10. Davarifar, M.; Rabhi, A.; El Hajjaji, A. Comprehensive Modulation and Classification of Faults and Analysis Their Effect in DC Side of Photovoltaic System. *Energy Power Eng.* **2013**, *5*, 230–236. [[CrossRef](#)]
11. Alam, M.K.; Khan, F.; Johnson, J.; Flicker, J. A comprehensive review of catastrophic faults in PV arrays: Types, detection, and mitigation techniques. *IEEE J. Photovolt.* **2015**, *5*, 982–997. [[CrossRef](#)]
12. Han, G.; Zhang, S.; Boix, P.P.; Wong, L.H.; Sun, L.; Lien, S.Y. Towards high efficiency thin film solar cells. *Elsevier Prog. Mater. Sci. J.* **2017**, *87*, 246–291.
13. Kumar, N.; Yadav, P.; Chandel, S.S. Comparative Analysis of Four Different Solar Photovoltaic Technologies. In Proceedings of the International Conference on Energy Economics and Environment (ICEEE), Noida, India, 26–28 March 2015.
14. Quansah, D.A.; Adaramola, M.S. Comparative study of performance degradation in poly- and mono-crystalline-Si solar PV modules deployed in different applications. *Int. J. Hydrogen Energy* **2018**, *43*, 3092–3109. [[CrossRef](#)]
15. Bostan, V.; Toma, A.R.; Tudorache, T.; Pațurcă, S.V.; Dumitrescu, A.M.; Bostan, I. Performance analysis of polycrystalline and CIS thin-film PV panels in real operation conditions. In Proceedings of the 2017 5th International Symposium on Electrical and Electronics Engineering, Galati, Romania, 20–22 October 2017; pp. 1–4.
16. Ozden, T.; Akinoglu, B.G.; Kurtz, S. Performance and Degradation Analyses of two Different PV Modules in Central Anatolia. In Proceedings of the 2018 International Conference on Photovoltaic Science and Technologies (PVCon), Ankara, Turkey, 4–6 July 2018; pp. 1–4.
17. Sharma, A.; Venkateswaran, V.B.; Singh, R. Experimental Analysis of Electrical and Thermal Effects of Various Configurations of Partial Shading on Three Different Solar Module Technologies. In Proceedings of the 2018 International Conference on Recent Trends in Electrical, Control and communication (RTECC), Malaysia, 20–22 March 2018; pp. 137–142.
18. Ahmed, J.; Salam, Z. A critical evaluation on maximum power point tracking methods for partial shading in PV systems. *Renew. Sustain. Energy Rev.* **2015**, *47*, 933–953. [[CrossRef](#)]
19. Velasco, G.; Guinjoan, F.; Pique, R. Grid-connected PV systems energy extraction improvement by means of an Electric Array Reconfiguration (EAR) strategy: Operating principle and experimental results. In Proceedings of the 2008 IEEE Power Electronics Specialists Conference, Rhodes, Greece, 15–19 June 2008; pp. 1983–1988.
20. Candela, R.; Di Dio, V.; Sanseverino, E.R.; Romano, P. Reconfiguration Techniques of Partial Shaded PV Systems for the Maximization of Electrical Energy Production. In Proceedings of the IEEE Conference on Clean Electrical Power, Capri, Italy, 21–23 May 2007; pp. 716–719.
21. Kumar, A.; Pachauri, R.K.; Chauhan, Y.K. Experimental analysis of SP/TCT PV array configurations under partial shading conditions. In Proceedings of the 2016 IEEE 1st International Conference on Power Electronics, Intelligent Control and Energy Systems (ICPEICES), Delhi, India, 4–6 July 2016; pp. 1–6.
22. Mehiri, A.; Hamid, A.K.; Almazrouei, S. The Effect of Shading with Different PV Array Configurations on the Grid-Connected PV System. In Proceedings of the 2017 International Renewable and Sustainable Energy Conference (IRSEC), Tangier, Morocco, 4–7 December 2017; pp. 1–6.
23. Pendem, S.R.; Mikkili, S. Performance evaluation of series, series-parallel and honey-comb PV array configurations under partial shading conditions. In Proceedings of the 2017 7th International Conference on Power Systems (ICPS), Pune, India, 21–23 December 2017; pp. 749–754.
24. Veerasamy, B.; Takeshita, T.; Jote, A.; Mekonnen, T. Veerasamy, Mismatch Loss Analysis of PV Array Configurations Under Partial Shading Conditions. In Proceedings of the 2018 7th International Conference on Renewable Energy Research and Applications (ICRERA), Paris, France, 14–17 October 2018; pp. 1162–1183.
25. Satpathy, P.R.; Jena, S.; Jena, B.; Sharma, R. Comparative study of interconnection schemes of modules in solar PV array network. In Proceedings of the International Conference on Circuit, Power and Computing Technologies (ICCPCT), Kollam, India, 20–21 April 2017; pp. 1–6.
26. Ramaprabha, R.; Mathur, B.L. Modeling and Simulation of Solar PV Array under Partial Shaded Conditions. In Proceedings of the IEEE Conference on Sustainable Energy Technologies, Singapore, 24–27 November 2008; pp. 7–11.
27. Nguyen, X.H. Matlab/Simulink based modeling to study effect of partial shadow on solar photovoltaic array. *Environ. Syst.* **2015**, *4*, 20. [[CrossRef](#)]
28. Zhao, Y.; De Palma, J.F.; Mosesian, J.; Lyons, R.; Lehman, B. Line-line fault analysis and protection challenges in solar photovoltaic arrays. *IEEE Trans. Ind. Electron.* **2013**, *60*, 3784–3795. [[CrossRef](#)]

29. Hua, C.C.; Ku, P.K. Implementation of a stand-alone photovoltaic lighting system with MPPT, battery charger and high brightness LEDs. In Proceedings of the 6th International Conference on Power Electronics and Drive Systems (PEDS'05), Kuala Lumpur, Malaysia, 28 November–1 December 2005.
30. Chan, F.; Calleja, H. Reliability: A new approach in design of inverters for PV systems. In Proceedings of the 10th IEEE International Power Electronics Congress (CIEP'06), Puebla, Mexico, 16–18 October 2006; pp. 97–102.
31. Pachauri, R.K.; Chauhan, Y.K. Hybrid PV/FC Stand Alone Green Power Generation: A Perspective for Indian Rural Telecommunication Systems. In Proceedings of the IEEE Conference on Issues and Challenges in Intelligent Computing Techniques, Ghaziabad, India, 7–8 February 2017; pp. 807–815.
32. Mathworks. Available online: <https://www.mathworks.com/help/phymod/sps/powersys/ref/pvarray.html> (accessed on 9 September 2019).
33. Villalva, M.G.; Gazoli, J.R.; Ruppert Filho, E. Comprehensive approach to modeling and simulation of photovoltaic arrays. *IEEE Trans. Power Electron.* **2009**, *24*, 1198–1208. [[CrossRef](#)]
34. Tan, R.H.; Hoo, L.Y. DC-DC converter modeling and simulation using state space approach. In Proceedings of the IEEE Conference on Energy Conversion (CENCON), Johor Bahru, Malaysia, 19–20 October 2015; pp. 42–47.



© 2019 by the authors. Licensee MDPI, Basel, Switzerland. This article is an open access article distributed under the terms and conditions of the Creative Commons Attribution (CC BY) license (<http://creativecommons.org/licenses/by/4.0/>).